

# Lentiviral-mediated *ephrin B2* gene modification of rat bone marrow mesenchymal stem cells

Journal of International Medical Research

2019, Vol. 47(7) 3282–3298

© The Author(s) 2019

Article reuse guidelines:

[sagepub.com/journals-permissions](http://sagepub.com/journals-permissions)

DOI: 10.1177/0300060519843023

[journals.sagepub.com/home/imr](http://journals.sagepub.com/home/imr)



Min Zhu , Yu Hua, Jian Tang, Xiaoke Zhao, Ling Zhang and Yue Zhang

## Abstract

**Objective:** To determine the effect of the upregulation or knockdown of the ephrinB2 (*Efnb2*) gene and the effect of EphB4/EphrinB2 signalling in rat bone marrow mesenchymal stem cells (BMSCs).

**Methods:** Rat BMSCs were infected with lentivirus vectors carrying EphrinB2 and shRNA-EphrinB2. EphrinB2 mRNA and protein levels were quantified. At 28 days of culture with neuronal cell-conditioned differentiation medium, levels of microtubule-associated protein 2 (MAP2), CD133 and nestin were detected in EphrinB2/BMSCs and shEphrinB2/BMSCs using quantitative polymerase chain reaction and immunofluorescence. The ability of these cells to migrate was evaluated using a transwell assay.

**Results:** BMSCs were successfully isolated as indicated by their CD90<sup>+</sup> CD29<sup>+</sup> CD34<sup>–</sup> CD45<sup>–</sup> phenotype. Three days after ephrinB2 transduction, BMSC cell bodies began to shrink and differentiate into neuron-like cells. At 28 days, levels of MAP2, CD133 and nestin, as well as the number of migratory cells, were higher in lenti-EphrinB2-BMSCs than in the two control groups. The shEphrinB2/BMSCs had reduced levels of MAP2, CD133 and nestin; and a lower rate of cell migration. Similarly, increased levels of Grb4 and p21-activated kinase in the EphB4/EphrinB2 reverse signalling pathway were observed by Western blot.

**Conclusions:** LV-EphrinB2 can be efficiently transduced into BMSCs, which then differentiate into neuron-like cells.

## Keywords

EphrinB2, EphB4, BMSCs, neural stem cells, migration

Date received: 5 November 2017; accepted: 18 March 2019

---

Department of Rehabilitation, Children's Hospital of Nanjing Medical University, Nanjing, Jiangsu Province, China

## Corresponding author:

Min Zhu, Department of Rehabilitation, Children's Hospital of Nanjing Medical University, 72 Guangzhou Road, Nanjing, Jiangsu Province, 210008, China.  
Email: 1553526445@qq.com



Creative Commons Non Commercial CC BY-NC: This article is distributed under the terms of the Creative Commons Attribution-NonCommercial 4.0 License (<http://www.creativecommons.org/licenses/by-nc/4.0/>) which permits non-commercial use, reproduction and distribution of the work without further permission provided the original work is attributed as specified on the SAGE and Open Access pages (<https://us.sagepub.com/en-us/nam/open-access-at-sage>).

## Introduction

Bone marrow mesenchymal stem cells (BMSCs) are precursor cells distinct from haematopoietic stem cells. Accumulating evidence from *in vitro* and *in vivo* studies suggests that BMSCs can differentiate into neuron-like cells under certain circumstances, such as the presence of inducers and cytokines that are consistent with embryonic neurogenesis, neural stem cell maturation and migration.<sup>1</sup> BMSCs *in vivo* have the ability to directly 'home' to damaged tissues and ischaemic regions for stem cell repair or replacement of necrotic structures.<sup>2</sup> Research has shown that erythropoietin-producing hepatocellular (Eph) receptors are the largest family of tyrosine kinase receptors.<sup>3</sup> Their ligands, the Eph family receptor-interacting proteins or Ephrins, are expressed mainly on the cell surface.<sup>4</sup> Both receptors and ligands are membrane-bound proteins that depend on each other for signal transduction.<sup>3</sup> They are involved in axon guidance, cell adhesion, and promotion of stem cell proliferation, differentiation, migration and angiogenesis, making them a focus of stem cell research.<sup>3</sup>

Erythropoietin-producing hepatocellular receptors can be divided into two groups: EphA (EphA1–EphA8, EphA10) and EphB (EphB1–EphB4, Eph B6).<sup>5</sup> Ephrin ligands are divided into two groups: EphrinA (EphrinA1–A5) and EphrinB (EphrinB1–3).<sup>5</sup> Currently, there are limited reports on the roles of EphB4 and EphrinB2 in stem cells.<sup>6</sup> Similar to other tyrosine kinase receptors, signal transduction between EphB4 and EphrinB2 is bidirectional, as each can be activated by the other, producing 'forward signals' and 'reverse signals'.<sup>3</sup> Autophosphorylation of the receptor is initiated by EphrinB2, with phosphoinositide 3-kinase, Src, mitogen-activated protein kinases, Akt and other proteins mediating the cascade reaction, thus giving rise to what is known as a

forward signal.<sup>5</sup> In contrast, the reverse signal is triggered when EphrinB2 binds to EphB4 as a ligand (Src-family kinases), a tyrosine residue of EphrinB2 is phosphorylated, and the downstream signalling pathway is activated by interaction with the SH2/SH3 domain of the adapter protein growth-factor-receptor-bound protein 4 (Grb4).<sup>3</sup> A previous study demonstrated that p21-activated kinase (PAK) acts as a key downstream component of ephrin-B3-Grb4 reverse signalling to mediate axon retraction and pruning.<sup>7</sup> The PDZ domain-binding C-terminus of EphrinB2 can interact with the PDZ domain of various proteins.<sup>5</sup> One of these, regulator of G-protein signalling 3 (PDZ-RGS3), acts downstream of EphrinB2 and is involved in regulating cell migration.<sup>5</sup> The EphrinB2 reverse signalling pathway for PDZ-RGS selectively promotes G protein-coupled stromal cell-derived factor 1 chemotaxis.<sup>8</sup> Forward signalling was shown to inhibit angiogenesis, preventing endothelial cell adhesion, migration, and vascular sprouting, whereas reverse signalling had the opposite effect.<sup>9</sup>

In this current study, the effects of lentiviral-mediated upregulation and knockdown of the ephrin B2 (*Efnb2*) gene on rat BMSC differentiation and cell migration, and the expression of phenotypic markers were investigated *in vitro*. In addition, the study explored the underlying molecular mechanisms involved in this process.

## Materials and methods

### Animals

Ten male specific pathogen-free Sprague–Dawley rats aged 4–6 weeks and weighing 160–200g obtained from the Experimental Animal Centre of Nanjing Medical University, Nanjing, Jiangsu Province, China were used in this study. Rats were

exposed to a 12-h light–dark cycle with free access to food and water. All animal experiments were approved by the Animal Care Committee in China and were performed according to institutional guidelines.

### *Isolation, purification, and identification of rat BMSCs*

Rats were sacrificed by cervical dislocation and placed in 75% ethanol for 5 min. Briefly, the bone marrow was obtained from the bilateral femurs and tibias, flushed out with 5 ml Dulbecco's modified Eagle's Medium (DMEM)/F12 (Gibco Life Technologies, Carlsbad, CA, USA) and mixed with equivalent percoll separating medium (1.073 g/l; Gibco Life Technologies). Following centrifugation at 900 *g* for 20 min at room temperature (Ultracentrifuge; Hitachi, Tokyo, Japan), the intermediate monolayer cells were collected and flushed twice with 10 mM phosphate-buffered saline (PBS; pH 7.4) for 3 min. The cell pellets were then added to complete cell culture medium containing a low-glucose solution of 89% Dulbecco's modified Eagle's medium (DMEM; HyClone, Logan, UT, USA), 10% fetal bovine serum (Corning, Corning, NY, USA) and 1% penicillin/streptomycin (Biyuntian, Shanghai, China). The mixture was suspended in lymphocyte separation medium (Gibco, Grand Island, NY, USA) and centrifuged for 20 min at 710 *g*. The third layer was extracted, placed into a 10 cm<sup>2</sup> culture dish with complete culture medium and cultured in an incubator at 37°C in an atmosphere of 5% CO<sub>2</sub> with saturated humidity. BMSCs from the third passage were collected and identified at 90% confluence. Conventional digestion, centrifugation, suspension, cell precipitation and three washes with 10 mM PBS (pH 7.4) resulted in a suspension of 1 × 10<sup>8</sup> cells/l. The cell suspension (100 μl) was incubated with 10 μl of fluorescently-labelled

antibodies: fluorescein isothiocyanate-conjugated anti-rat CD29, allophycocyanin-conjugated anti-rat CD45, phycoerythrin-conjugated anti-rat CD90, and electron coupled dye-conjugated anti-rat CD34 (1:100 dilution; all from Becton Dickinson, Franklin Lakes, NJ, USA) for 30 min at 4°C in the dark, respectively. Washed cells were identified following detection of specific markers by flow cytometry using a COULTER® EPICS® XL™ Flow Cytometer (Beckman Coulter, Brea, CA, USA).

### *Preparation of lentiviral vectors*

The *Efnb2* gene overexpression lentivirus was constructed and termed LV-EphrinB2. The *Efnb2* gene was amplified from rat cDNA. Total RNA (1 μg) was extracted from BMSCs at 1 week using an RNA Extraction kit (Invitrogen, Carlsbad, CA, USA) according to the manufacturer's instructions. cDNAs were produced using a PrimeScript™ RT Reagent Kit (Takara, Dalian, China). Reverse transcription (RT) was carried out using a Step OnePlus™ Real-Time PCR System (Applied Biosystems, Foster City, CA, USA) with Syber Green PCR Master Mix (Applied Biosystems) based on the company's guidelines under the following conditions: preliminary denaturation at 95°C for 3 min, followed by 30 cycles of denaturation at 95°C for 30 sec, annealing at 60°C for 30 sec and elongation at 72°C for 90 sec, with a final elongation step at 72°C for 10 min using a GeneAmp® PCR System 9700 thermal cycler (Applied Biosystems). To amplify the *Efnb2* gene using polymerase chain reaction (PCR), the following pairs of primers were designed and synthesized (Genechem Biotech, Shanghai, China): forward: 5'-CAGGTCGACTCTAGAGGATCCCGCCACCATGGCCATGGCCCGGTCCAGGAG-3'; reverse: 5'-ATAGCGCTACCCGGGGATCCGACCTTGTAGTA

AATGTTGGCAG-3'. The resulting *Efnb2* cDNA was inserted into the lentiviral vector GV416 (sequence elements: EF1 $\alpha$ -MCS-3FLAG-CMV-EGFP-T2A-Puromycin; Shanghai Genechem Company, Shanghai, China) to create the lentiviral vector GV416-EphrinB2. The recombinant and two lentiviral helper plasmids were co-transduced (Helper 1.0 and Helper 2.0; Shanghai Genechem Company) into 293T cells to generate the target lentivirus with an infectious viral titre of  $1 \times 10^9$  TU/ml, which was measured using a fluorescence assay method. In parallel, a negative lentivirus was produced by co-transducing the lenti-green fluorescent protein (GFP) empty vector GV416 with GFP but without *Efnb2* and two lentiviral helper plasmids (Helper 1.0 and Helper 2.0) into 293T cells, yielding an infectious viral titre of  $1 \times 10^9$  TU/ml. The titre of the virus was determined by the dilution method, after which the prepared lentiviral vector was stored at  $-80^\circ\text{C}$ . The *Efnb2* gene silencing lentiviral vector was also constructed and termed LV-short hairpin (sh)

RNA-EphrinB2. A total of three target shRNAs (shRNA1, shRNA2 and shRNA3) and one negative scrambled shRNA (EphrinB2-rat-NC), as listed in Table 1, were designed using siRNA Target Finder and Design Tools software (Shanghai Genechem Company). The cloned DNA segment was inserted into the lentiviral vector pHBLVU6 (sequence elements: pHBLV-U6-MCS-CMV-ZsGreen-PGK-PURO). Sequence analysis confirmed that the inserted *Efnb2* gene and shRNA-EphrinB2 sequences were correct. To screen for specific small interfering (si)RNAs against EphrinB2 mRNA, 293T cells were co-transfected with LV-shRNA1/2/3-EphrinB2, respectively. The successfully constructed lentiviral vector and packaging plasmid (mix) were co-transfected into the 293T cells using Lipofectamine 2000 (Invitrogen). Packaging and titration of the lentiviral vectors were performed. After transfection for 8 h, the culture medium was changed to complete medium. The supernatant was harvested after culturing for 48 h and

**Table 1.** Short hairpin (sh)RNA sequences of EphrinB2.

Name	Sequence
shRNA1 Top strand	GATCCGATCGATAGTTCTAGAGCCTATCTATTCAAGAGATAGATAGGCTCTAGAACTATCGATCTTTTTTC
shRNA1 Bottom strand	AATTGAAAAAGATCGATAGTTCTAGAGCCTATCTATCTCTTG AATAGATAGGCTCTAGAACTATCGATCG
shRNA2 Top strand	GATCCGAGCAAGCCGACAGATGCACTATTATTCAAGAGATAATAGTGCATCTGTCGGCTTGCTCTTTTTTC
shRNA2 Bottom strand	AATTGAAAAAGAGCAAGCCGACAGATGCACTATTATCTCTTGAATAATAGTGCATCTGTCGGCTTGCTCG
shRNA3 Top strand	GATCCGCAGACAGTGTCTTCTGCCACACTATTCAAGAGATAGTGTGGCAGAAGACACTGTCTGTTTTTTC
shRNA3 Bottom strand	AATTGAAAAACAGACAGTGTCTTCTGCCACACTATCTCTTGAATAGTGTGGCAGAAGACACTGTCTGCG
shRNA-NC Top strand	GATCCGTTCTCCGAACGTGTCACGTAATTCAAGAGATTACGTGACACGTTCCGAGAATTTTTTC
shRNA-NC Bottom strand	AATTGAAAAATTCTCCGAACGTGTCACGTAATCTCTTGAATTA CGTGACACGTTCCGAGAACG

concentrated by ultrafiltration. The virus titre was measured using the dilution gradient method and calculated as follows: virus titre (TU/ml) = counted fluorescent cells / corresponding volume of virus stock solution. Ultimately, the titre of the lentivirus was  $1 \times 10^9$  TU/ml and the lentivirus was stored at  $-80^\circ\text{C}$  for later use.

### Lentivirus transduction

Rat BMSCs were cultured for three generations and then seeded into 24-well plates at a density of  $1 \times 10^5$  cells/well. The cells were cultured for 2 or 3 days, whereby the cell fusion rate was approximately 50%. Viruses at multiplicity of infection (MOI) rates of 10 and 20 were added together with 5  $\mu\text{g/ml}$  polybrene. To establish EphrinB2-BMSCs, the lenti-EphrinB2-GFP or lenti-GFP empty vector was used to transduce naive BMSCs at passage 5 (MOI = 10 and 20). In the negative-transduction group, the lenti-GFP empty vector was used. The no-transduction control group was not treated at all. After transduction for 24–48 h, enhanced green fluorescent protein (EGFP) levels were observed every day using a BX41 upright fluorescence microscope (Olympus, Tokyo, Japan) and transduction efficiency was determined.

After transduction, four groups were set up: control group (no transduction, other culture conditions were the same as those used for the transduction groups), NC group (negative control group, transduced with lenti-GFP empty vector), lenti-10moi-EphrinB2-GFP group (transduced with lenti-EphrinB2-GFP at a MOI of 10), and lenti-20moi-EphrinB2-GFP group (transduced with lenti-EphrinB2-GFP at a MOI of 20). Each group was tested in triplicate.

Third-passage BMSCs were transduced with no lentiviral vector, negative control lentiviral vector, and LV-shRNA1-EphrinB2, LV-shRNA2-EphrinB2, LV-shRNA3-EphrinB2, with a MOI of 20,

and 5  $\mu\text{l}$  polybrene (10mg/ml) was added, respectively. The stable control, negative control group, and EphrinB2-knockdown cell lines, termed BMSCs, GFP/BMSCs, and EphrinB2-shRNA1/BMSCs, EphrinB2-shRNA2/BMSCs and EphrinB2-shRNA3/BMSCs, were established in culture medium containing puromycin (5  $\mu\text{l/ml}$ ).

### Quantitative PCR (qPCR) analysis of EphrinB2 mRNA levels in BMSCs

To determine the abundance of EphrinB2 mRNA, total RNA was extracted from cells using an RNA Extraction kit (Invitrogen). Based on the company's protocol, cDNAs were synthesized from 0.1 mg of total RNA using a PrimeScript™ RT Reagent Kit (Takara). RT was carried out using a Step OnePlus™ Quantitative Real-Time PCR System (Applied Biosystems) with Syber Green PCR Master Mix (Applied Biosystems) according to the manufacturer's guidelines under the following conditions: preliminary denaturation at  $95^\circ\text{C}$  for 3 min, followed by 30 cycles of denaturation at  $95^\circ\text{C}$  for 30 sec, annealing at  $56^\circ\text{C}$  for 45 sec and elongation at  $72^\circ\text{C}$  for 45 sec, with a final elongation step at  $72^\circ\text{C}$  for 10 min using a GeneAmp® PCR System 9700 thermal cycler (Applied Biosystems). The following qRT-PCR primer sequences were used (Genechem Biotech): for the internal control glyceraldehyde 3-phosphate dehydrogenase (GAPDH) forward: 5'-GTGAGGTGACCGCATCTTCT-3', GAPDH reverse: 5'-CTTGCCGTGGGT AGAGTCAT-3', for a PCR product of 353 base pairs (bp); and for EphrinB2 forward: 5'-GACGTCCAGA ACTAGAAGCTGG-3', EphrinB2 reverse: 5'-CACCATCCAATGGAAGC CTGG-3', for a PCR product of 257 bp. Data were normalized to GAPDH and calculated using the  $2^{-\Delta\Delta\text{Ct}}$  method. All samples



normalized with GAPDH level, as the loading control.

### **Western blot analysis of EphrinB2 protein levels in BMSCs**

Total cellular protein was extracted 48 h after transduction and the protein concentration was measured using a BCA kit (Solarbio, Shanghai, China). Total protein (30 µg) was boiled with 2 × loading buffer at 95 °C for 10 min. Samples were then separated by 15% sodium dodecyl sulphate–polyacrylamide gel electrophoresis and electrophoretically transferred to a polyvinylidene fluoride membrane (Millipore, Billerica, MA, USA) at 100 V for 45–70 min. Then, the membrane was blocked with 5% bovine serum albumin (BSA) for 1 h at room temperature, followed by incubation with a rabbit polyclonal anti-EphrinB2 primary antibody (1:200 dilution; Abcam, Cambridge, UK) at 4 °C overnight. The blots were then rinsed three times with tris-buffered saline-Tween 20 (TBS-T; pH 7.6) for 5 min followed by incubation with horseradish peroxidase-conjugated goat anti-rabbit secondary antibody (1:5000 dilution; Solarbio) at room temperature for 1 h. After washing the membrane three times for 5 min each with TBS-T (pH 7.6), the blots were developed by chemiluminescence followed by imaging with a Bio-Rad Geldoc EZ formatter (Bio-Rad Laboratories, Hercules, CA, USA). All membranes were incubated also with a monoclonal anti-GAPDH antibody (1:1000 dilution; Santa Cruz Biotechnology, Santa Cruz, CA, USA) as an internal reference control. Band intensity was quantified by ImageJ software (NIH, Bethesda, MD, USA). GAPDH was used as loading control. The levels of EphrinB2 protein were detected using Western blotting and the most effective siRNAs were used for further investigation.

### **Differentiation of BMSCs into neural-like stem-like cells in vitro**

The potential of rat BMSCs to differentiate into neural-like stem cells was analysed. To induce BMSC differentiation, third-passage BMSCs were collected, and 0.25% trypsin was added to digest the cells for 10 min. Supernatants were obtained and pancreatin was subsequently removed. The cells were resuspended in neuronal cell-conditioned differentiation medium containing 60 g/l glucose, 20 g/l basic fibroblast growth factor (FGF), 20 g/l epidermal growth factor (EGF) and 2% B27 DMEM/F12 (1:1) at a density of  $5 \times 10^7$  cells/l. The medium was changed based on cell growth. Cell morphology was observed directly using phase-contrast microscopy (BX41; Olympus). Cells were cultured in 24-well plates and then fixed with 4% paraformaldehyde at 20 °C. To analyse the effects of the increased levels of EphrinB2 protein on BMSC differentiation, the third-passage BMSCs were divided into four groups: control group, NC group, lenti-10moi-EphrinB2-GFP group and lenti-20moi-EphrinB2-GFP group. The morphology of the BMSCs and the levels of specific neural markers, including microtubule-associated protein 2 (MAP2), CD133 and nestin in each group were observed using a BX41 upright fluorescence microscope (Olympus). After 28 days of culture, positive induction was detected by immunofluorescence staining. Cells were washed with 10 mM PBS (pH 7.4) and permeabilized with 0.2% Triton X-100 for 5 min. After washing with 10 mM PBS (pH 7.4), cells were incubated in a blocking buffer containing 5% BSA for 30 min at 20 °C, followed by incubation with anti-MAP2 (1:500 dilution; Proteintech, Chicago, IL, USA), anti-CD133 (1:500 dilution; Abcam), and anti-nestin (1:500 dilution; Abcam) antibodies overnight at 4 °C. Secondary antibodies labelled with

fluorescein (1:500 dilution, Abcam) were applied for 120 min at room temperature. After incubation with 0.1% 2-(4-amidinophenyl)-6-indolecarbamide dihydrochloride for 5 min, cells were washed with 10 mM PBS (pH 7.4) three times. Images were captured on a wide-field BX41 upright fluorescence microscope (Olympus). The mean fluorescence intensity of MAP2, CD133 and nestin was analysed using ImageJ software (NIH).

The level of MAP2 mRNA was detected using semi-quantitative PCR. Total RNA was extracted from cells using an RNA Extraction kit (Invitrogen). Based on the manufacturer's instructions, cDNAs were synthesized from 0.1 mg of total RNA using a PrimeScript™ RT Reagent Kit (Takara). RT was carried out using a Step OnePlus™ Quantitative Real-Time PCR System (Applied Biosystems) with Syber Green PCR Master Mix (Applied Biosystems) based on the manufacturer's instructions under the following conditions: preliminary denaturation at 95°C for 3 min, followed by 30 cycles of denaturation at 95°C for 30 sec, annealing at 56°C for 45 sec and elongation at 72°C for 45 sec, with a final elongation step at 72°C for 10 min using a GeneAmp® PCR System 9700 thermal cycler (Applied Biosystems). The following qRT-PCR primer sequences were used (Genechem Biotech): for the internal control GAPDH forward: 5'-GTGAGG TGACCGC ATCTTCT-3', GAPDH reverse: 5'-CTTGCCGT GGGTAGAGTC AT-3', for a PCR product of 353 bp; and for MAP2 forward: 5'-ACCTTCCTCCATCC TCCCTC-3', MAP2 reverse: 5'-AGTAGG TGTT GAGGTGCCGC-3', for a PCR product of 151 bp. Data were normalized to GAPDH and calculated using the  $2^{-\Delta\Delta C_t}$  method. All samples normalized with GAPDH level, as the loading control.

To analyse the effects of the silencing of EphrinB2 on BMSC differentiation, third-passage BMSCs were divided into three

groups: control group, NC group (transduced with negative control lentiviral vector) and shEphrinB2 (transduced with LV-shRNA- EphrinB2), which were all induced by neuronal cell-conditioned differentiation medium containing 60 g/l glucose, 20 g/l basic FGF, 20 g/l EGF and 2% B27 DMEM/F12 (1:1) at a density of  $5 \times 10^7$  cells/l. The levels of MAP2, CD133 and nestin proteins were detected using cell immunofluorescence and Western blotting. The mRNA levels of MAP2 was detected using semi-quantitative PCR. The morphology of the BMSCs was observed using a BX41 upright fluorescence microscope (Olympus). The mean fluorescence intensity of MAP2, CD133 and nestin was analysed using ImageJ software (NIH).

### Cell migration assay

The cell migration assay was performed in a transwell chamber that contained a polyethylene terephthalate track-etched membrane with 8.0- $\mu$ m pores. Briefly, 0.5-ml suspensions of LV-EphrinB2-BMSCs/shRNA-EphrinB2-BMSCs or control BMSCs at a concentration of  $1 \times 10^5$  cells/ml were added to the top of the chamber layer. In the bottom chamber, different concentrations of murine hepatocyte growth factor (Peprotech, Rocky Hill, NJ, USA) were used as a chemoattractant. The cells in the transwell chambers were incubated in a humidified tissue culture incubator overnight at 37°C and an atmosphere of 5% CO<sub>2</sub>. After 24 h, the cells were fixed and stained with 4% paraformaldehyde and 0.1% crystal violet, respectively. Migrated cells were observed, imaged and counted within three fields using a BX41 upright fluorescence microscope (Olympus).

### Western blot analysis

To reveal the mechanisms underlying EphrinB2-associated regulation,

phosphorylation of key kinases in the EphB4/EphrinB2 reverse signalling pathway in BMSCs was evaluated following inducing increased levels of EphrinB2. The Western blot assay was performed as described above for EphrinB2. Briefly, membranes were incubated at 4°C overnight with primary antibodies against intracellular PAK1 (PAK1; 1:1000 dilution; ab131522), phosphorylated PAK1 (p-PAK1; 1:1000 dilution; ab75599), Grb4 (1:1000 dilution; ab80620; all from Abcam) or GAPDH (1:1000 dilution; Santa Cruz Biotechnology). The membranes were then incubated with the corresponding secondary antibodies. The blots were developed using enhanced chemiluminescence Western blotting reagents and visualized using the Bio-Rad Image Lab system (Bio-Rad Laboratories).

### Statistical analyses

All statistical analyses were performed using IBM SPSS Statistics for Windows, Version 19.0. (IBM Corp., Armonk, NY, USA). Data are expressed as the mean  $\pm$  SE. Differences among groups were evaluated by one-way analysis of variance, followed by least significant difference (LSD) tests. A  $P$ -value  $< 0.05$  was considered statistically significant.

## Results

Ten samples of third-passage cells were examined by flow cytometry. The cells were negative for CD34 and CD45 and positive for CD29 and CD90, which indicated that they were not haematopoietic stem cells. The cultured rat BMSCs conformed to the characteristics of mesenchymal stem cells and were highly pure (Figure 1).

Enhanced green fluorescent protein was observed under an inverted fluorescence microscope and transduction efficiency was determined. Lenti-EphrinB2-BMSCs

showed green fluorescence at 24 h, but the number of EGFP-positive cells was small and the fluorescence was weak. At intervals of 1 day, infections were repeated, and the number of EGFP-positive cells increased, leading to enhanced fluorescence at 72 h. Therefore, the levels of EphrinB2 was evaluated at this time.

Quantitative PCR showed that the levels of EphrinB2 mRNA in the NC group were not significantly different from those in the control group (Figure 2A). The transcript levels of EphrinB2 mRNA in lenti-EphrinB2-BMSCs were significantly higher than those in the control and NC group ( $P < 0.05$  for all comparisons). The level of EphrinB2 mRNA was significantly higher in the lenti-20moi-EphrinB2-GFP group than in the lenti-10moi-EphrinB2-GFP group ( $P < 0.05$ ).

Western blot analysis revealed no significant difference in the levels of EphrinB2 protein between the control and NC groups (Figure 2B). The levels of EphrinB2 protein in the lenti-EphrinB2-BMSCs were significantly higher than those in the control and NC groups ( $P < 0.05$  for all comparisons). The levels of EphrinB2 protein were significantly higher in the lenti-20moi-EphrinB2-GFP group than in the lenti-10moi-EphrinB2-GFP group ( $P < 0.05$ ).

At a MOI of 20, the number of EGFP-positive cells and fluorescence intensity were optimal, and there was no obvious effect of transduction on the morphology of BMSCs (Figure 2C). The transduction rates in the lenti-EphrinB2-BMSCs were significantly different from those in the control and the NC groups ( $P < 0.05$  for all comparisons).

Quantitative PCR and Western blot analysis revealed that LV-shRNA3-EphrinB2 was the most effective siRNA against EphrinB2 (Figures 2D and 2E) so it was used for the subsequent investigations. Western blot analysis demonstrated



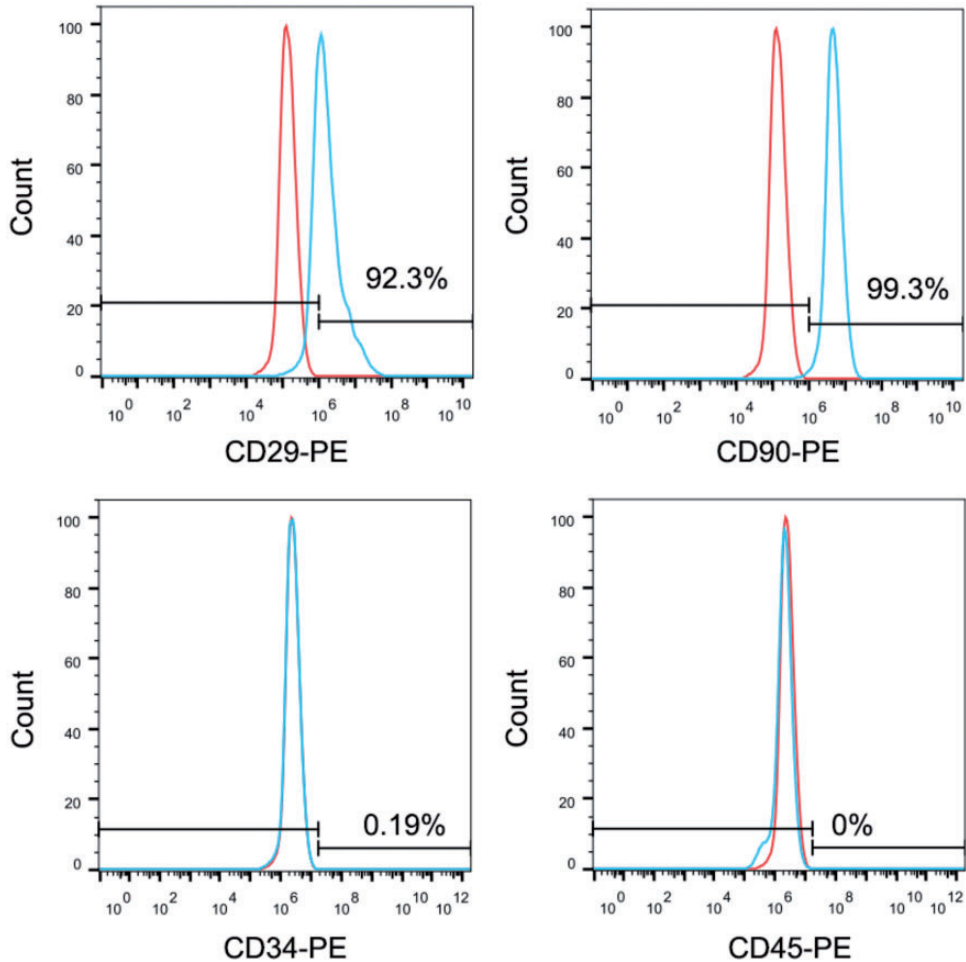


**Figure 1.** Identification of rat bone marrow mesenchymal stem cells (BMSCs) using flow cytometry. Isolated BMSCs were incubated with fluorescently-labelled antibodies against CD29, CD90, CD34, or CD45, followed by flow cytometry assessment. Cells were positive for the stem cell markers CD29 and CD90 and negative for the haematopoietic stem cell markers CD34 and CD45.

that EphrinB2 protein was detected in the control and NC groups, but not in the LV-shRNA-EphrinB2 groups, suggesting that the shEphrinB2/BMSC line was successfully established. The BMSCs exhibited a neuronal phenotype in the control and NC groups. However, the majority of BMSCs exhibited no marked morphological changes (Figure 2F) in the LV-shRNA-EphrinB2 group.

Three days after EphrinB2 gene transduction, partial retraction of the cytoplasm to the nucleus occurred in the four groups following addition of the inducer. Furthermore, the cell bodies were reduced in size, irregular or rounded in shape, with three-dimensional, surrounding strong refraction. Frequently, several short projections and a longer projection were observed. Neuron-like cells exhibited a

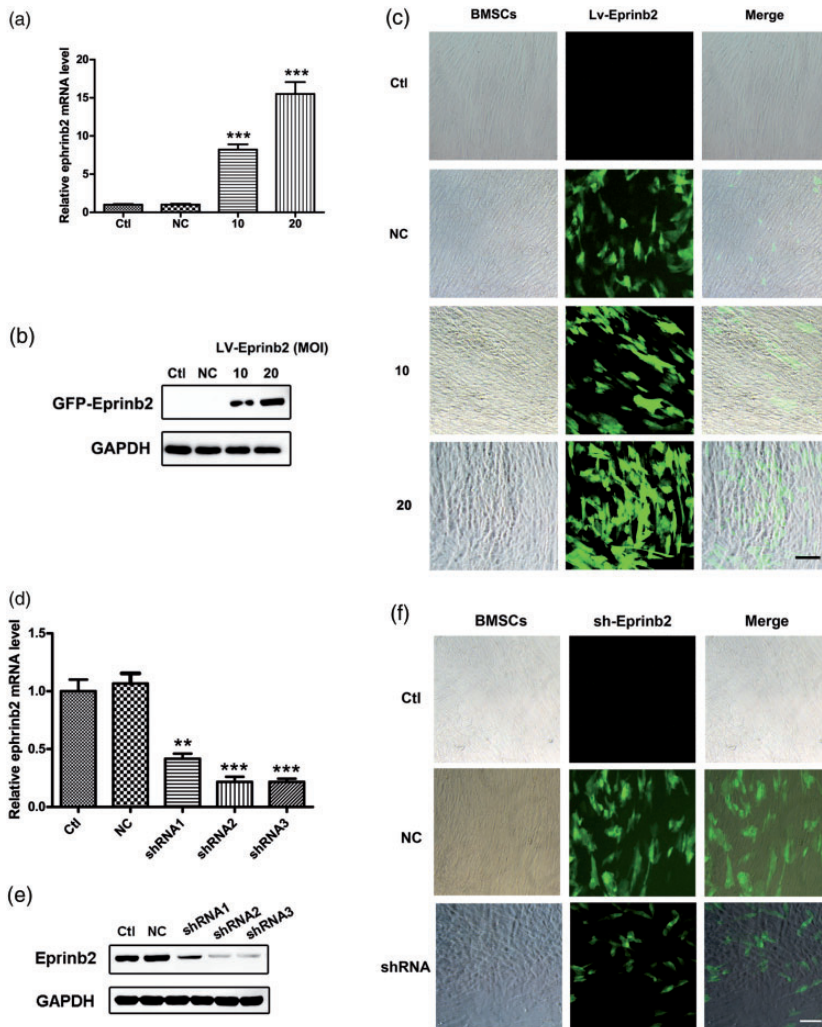


**Figure 2.** Upregulation and knockdown of EphrinB2 in rat bone marrow mesenchymal stem cells (BMSCs) transduced with the lenti-EphrinB2-GFP vector and LV-shRNA-EphrinB2. (A) Quantitative polymerase chain reaction (PCR) demonstrated that the levels of EphrinB2 mRNA were significantly increased in the LV-EphrinB2 group compared with the control (Ctl) and negative control (NC) groups. (B) Western blot analysis demonstrated that the levels of EphrinB2 protein were increased in the LV-EphrinB2 group compared with the Ctl and NC groups. (C) BMSCs were observed using microscopy (magnification  $\times 400$ ) and it was revealed that BMSCs exhibited a neuronal phenotype following transduction with LV-EphrinB2. (D) Quantitative PCR detected that LV-shRNA3-EphrinB2 was the most effective siRNA against EphrinB2. (E) Western blot analysis demonstrated that LV-shRNA3-EphrinB2 was the most effective siRNA against EphrinB2. Western blot analysis revealed that the levels of the EphrinB2 protein were significantly decreased in the LV-shRNA-EphrinB2 group compared with the Ctl and NC groups. (F) BMSCs exhibited a neuronal phenotype in the Ctl and NC groups; however, the majority of BMSCs exhibited no marked morphological changes. Scale bar 50  $\mu$ m. All data shown represent the mean  $\pm$  SEM of at least three independent experiments. \* $P < 0.05$  versus the Ctl and NC groups;  $^{\#}P < 0.05$  versus the lenti-10moi-EphrinB2-GFP (10) group;  $^{\Delta}P < 0.05$  versus the LV-shRNA1-EphrinB2 group. GAPDH, glyceraldehyde 3-phosphate dehydrogenase; loading control. The colour version of this figure is available at: <http://imr.sagepub.com>.

typical bipolar, multi-polar and tapered shape with a strong refraction. The neuron-specific markers MAP2, CD133, and nestin were used to stain the induced BMSCs. After adding 5  $\mu\text{g/l}$  FGF and EGF at 28 days after transduction, cell immunofluorescence analysis revealed that the levels of MAP2, CD133 and nestin were significantly higher in lenti-EphrinB2-BMSCs than in the control and NC groups ( $P < 0.05$  for all comparisons).

There was no statistically significant difference in the levels of MAP2, CD133 and nestin between the lenti-10moi-EphrinB2-GFP group and the lenti-20moi-EphrinB2-GFP group (Figures 3A–3C). According to semi-quantitative PCR, the BMSCs exhibited significantly higher levels of MAP2 mRNA in the lenti-20moi-EphrinB2-GFP group compared with in the control and NC groups ( $P < 0.05$ ; Figure 3D).

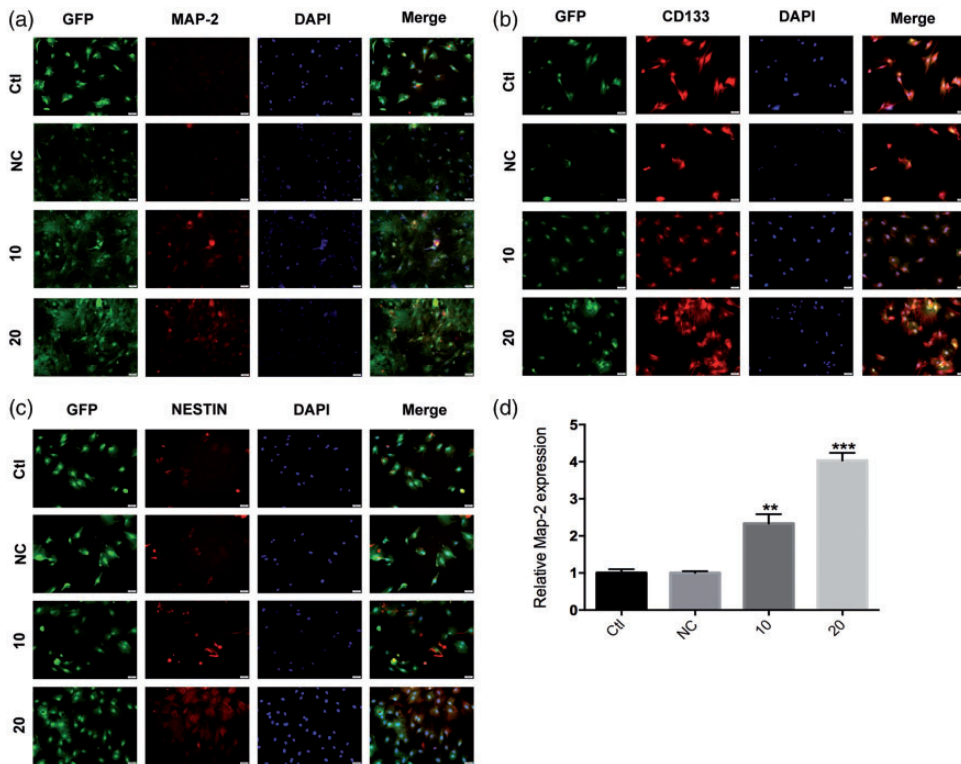


**Figure 3.** Upregulation of EphrinB2 promotes the differentiation of rat bone marrow mesenchymal stem cells (BMSCs) into neuron-like cells. The ability of BMSCs to differentiate into neuron-like cells was significantly enhanced when EphrinB2 was upregulated in BMSCs. (A–C) BMSCs were stained positive for specific neural markers including microtubule-associated protein 2 (MAP2), CD133 and nestin in the LV-EphrinB2 groups under induction conditions as determined using immunofluorescence analysis. (D) Semi-quantitative polymerase chain reaction revealed that the levels of MAP2 mRNA were increased in lenti-EphrinB2-BMSCs compared with the control (Ctl) and negative control (NC) groups. Scale bar 50  $\mu\text{m}$ . All data shown represent the mean  $\pm$  SEM of at least three independent experiments. \* $P < 0.05$  versus the Ctl group; \*\* $P < 0.05$  versus the lenti-10moi-EphrinB2-GFP (10) group. GFP, green fluorescent protein; DAPI, 2-(4-amidinophenyl)-6-indolecarbamide dihydrochloride. The colour version of this figure is available at: <http://imr.sagepub.com>.

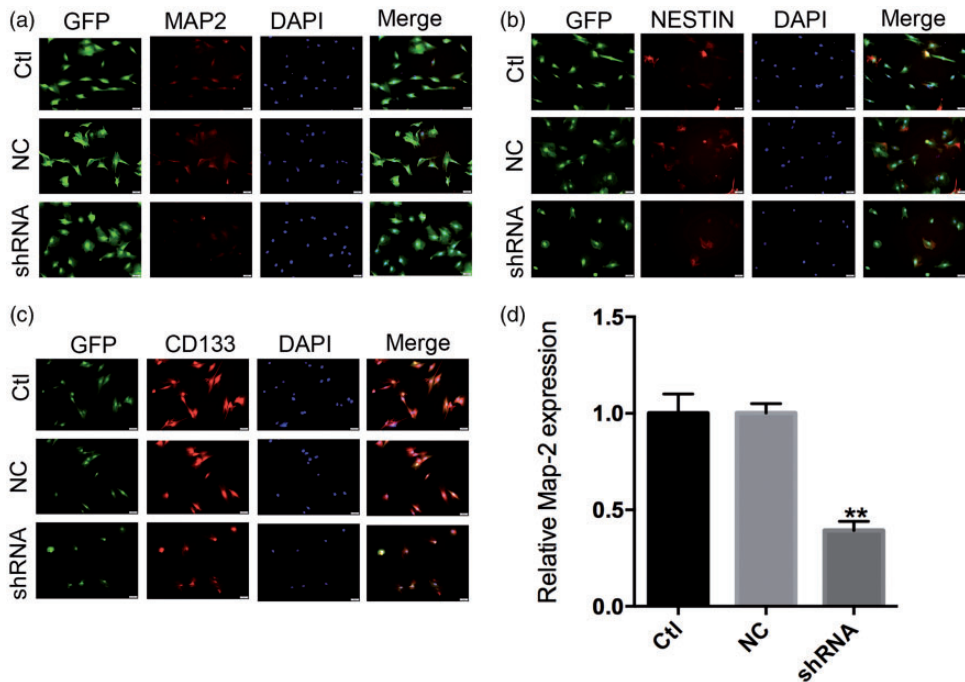


**Figure 4.** Ability of rat bone marrow mesenchymal stem cells (BMSCs) to differentiate into neuron-like cells is significantly reduced when the production of EphrinB2 in BMSCs is inhibited. (A–C) Immunofluorescence analysis demonstrated that the levels of microtubule-associated protein 2 (MAP2), CD133 and nestin were decreased in the LV-shRNA-EphrinB2 group compared with the control and NC groups under induction conditions. (D) Semi-quantitative polymerase chain reaction detection revealed that the levels of MAP2 mRNA were decreased in the LV-shRNA-EphrinB2 group compared with the control (Ctl) and negative control (NC) groups. Scale bar 50  $\mu$ m. All data shown represent the mean  $\pm$  SEM of at least three independent experiments. \* $P < 0.05$  versus the Ctl and NC groups. GFP, green fluorescent protein; DAPI, 2-(4-amidinophenyl)-6-indolecarbamide dihydrochloride. The colour version of this figure is available at: <http://imr.sagepub.com>.

Following induction by neuronal cell-conditioned differentiation medium, the BMSCs exhibited a neuronal phenotype in the control and NC groups; however, the majority of BMSCs exhibited no marked morphological changes in the LV-shRNA-EphrinB2 group, suggesting that neuron-like cells were successfully induced by neuronal cell-conditioned differentiation medium. Cell immunofluorescence analysis revealed that the levels of MAP2, CD133 and nestin were significantly reduced in the LV-shRNA-EphrinB2 group compared with the control and NC groups ( $P < 0.05$

for all comparisons; Figures 4A–4C). In addition, according to semi-quantitative PCR, the mRNA levels of MAP2 were significantly reduced in the LV-shRNA-EphrinB2 group compared with the control and NC groups ( $P < 0.05$  for both comparisons; Figure 4D).

Transwell experiments were conducted to investigate the effect of EphrinB2 on the migration of stem cells (Figure 5A). The mean  $\pm$  SEM number of migrated cells per field in the lenti-10moi-EphrinB2-GFP group ( $130.18 \pm 8.57$  cells) and lenti-20moi-EphrinB2-GFP group ( $142.32 \pm 6.53$  cells)

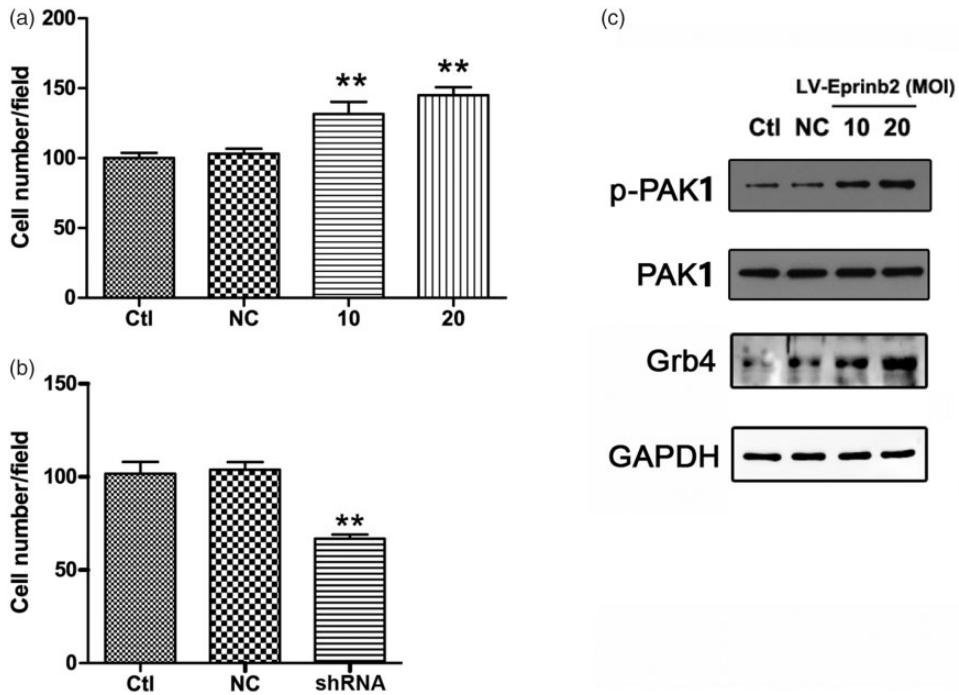


**Figure 5.** Effect of EphrinB2 on the migration of rat bone marrow mesenchymal stem cells (BMSCs) by activating the p21-activated kinase (PAK) signalling through modulating Grb4. (A) Transwell migration assays of EphrinB2-BMSCs versus control BMSCs (control [Ctl] and negative control [NC]). (B) Transwell migration assays of LV-shRNA-EphrinB2-BMSCs versus control BMSCs (Ctl and NC). (C) Phosphorylation of key kinases in the PAK and Grb4 pathway was investigated using Western blot analysis. All data shown represent the mean  $\pm$  SEM of at least three independent experiments. \* $P < 0.05$  versus the Ctl and NC groups. GAPDH, glyceraldehyde 3-phosphate dehydrogenase; loading control.

was significantly higher than that in the control group ( $101.02 \pm 4.32$  cells) and NC group ( $102.25 \pm 5.08$  cells) ( $P < 0.05$  for all comparisons). There was no significant difference in migration between the control and NC groups. These results showed that EphrinB2-BMSCs could migrate more efficiently than control BMSCs *in vitro*.

To obtain further evidence that EphrinB2 is important in BMSC migration, *Efnb2* gene expression in BMSCs was knocked down using siRNA. After treatment with shRNA-EphrinB2, a marked decrease in the number of migrated cells was observed (Figure 5B). The mean

$\pm$  SEM number of migrated cells per field in the LV-shRNA-EphrinB2- group ( $63.58 \pm 4.53$  cells) was significantly lower than that in the control group ( $101.36 \pm 6.21$  cells) and NC group ( $102.01 \pm 5.16$  cells) ( $P < 0.05$  for both comparisons). There was no significant difference in migration between the control and NC groups. These results show that shEphrinB2-BMSCs migrated less efficiently than control BMSCs *in vitro*.

The protein levels of Grb4, PAK and phosphorylated PAK were upregulated by Ephrin B2 upregulation, suggesting that EphrinB2 can activate the PAK signalling pathway by modulating Grb4 (Figure 5C).



## Discussion

This current study investigated the effects of lentiviral-mediated upregulation and knockdown of the *Efnb2* gene on rat BMSC differentiation, cell migration, expression of phenotypic markers and the underlying molecular mechanisms involved in EphB4/EphrinB2 signalling during these processes. The results demonstrated that upregulation of EphrinB2 promoted the differentiation of BMSCs into neuron-like cells and enhanced their migration in a transwell-based assay. The ability of BMSCs to differentiate into neuron-like cells and to migrate was significantly reduced when the production of EphrinB2 in BMSCs was inhibited.

Bone marrow mesenchymal stem cells have the ability to regenerate and differentiate.<sup>10</sup> Furthermore, they are easy to obtain and expand *in vitro*. Indeed, *in vitro* studies have shown that BMSCs can be induced to differentiate into nerve-like cells and vascular endothelial cells under specific conditions, which makes BMSCs ideal carrier cells for gene therapy for central nervous system diseases.<sup>10</sup>

Recent studies have defined the roles of EphB4/EphrinB2 and shown that their bidirectional signalling is important in neuronal cell differentiation, adhesion and migration and for stem cell transplantation.<sup>5</sup> EphrinB2 is derived from the Eph family, which is the largest subfamily of receptor tyrosine kinases.<sup>3</sup> EphB4 and EphrinB2 are both transmembrane proteins. EphB4 contains three parts: an extracellular region containing an N-terminal ligand domain, which is rich in cysteines and two type III fibronectins; a cell membrane region; and an intracellular region containing a tyrosine kinase domain, a highly conserved SAM domain, and a PDZ domain.<sup>5</sup> EphrinB2 also contains three parts: an intracellular region with a conserved C tail (the binding site for tyrosine kinases) and a PDZ domain, a cell

membrane region, and an extracellular region that binds its receptor through glycosylphosphatidylinositol.<sup>5</sup> EphrinB proteins can also have PDZ- and SH2-independent functions, some of which presumably depend on the SH3 domain of associating proteins (e.g. GRB4).<sup>5,11</sup> EphrinB2 binding to the Eph receptor via this extracellular portion activates phosphorylation of the tyrosine kinase binding site on Eph-expressing cells, leading to activation of downstream pathways.<sup>12</sup> Simultaneously, phosphorylation of tyrosine kinase occurs within the cell, and the downstream portion of the pathway is activated for unique bidirectional Eph–Ephrin signalling.<sup>5</sup> This bidirectional signalling can play an important role in cell repulsion and adhesion.<sup>13</sup> Significant progress has been made in understanding the role of EphrinB2 expression during the embryonic stage.<sup>14</sup> A previous study reported the role of EphrinB2 in inducing vascular endothelial cell migration during this stage.<sup>14</sup> Related literature also shows that EphrinB2 can induce the migration of spinal nerve cells at the embryonic stage and promote the development of many organs, including those in the olfactory systems.<sup>15–18</sup> Another study found that  $\gamma$ -secretase promoted migration by stimulating the reverse EphrinB2 signalling pathway in microglia derived from mouse embryonic stem cells.<sup>19</sup> At present, although there is some controversy over the role of EphrinB2 in angiogenesis and migration, most studies have suggested that the reverse signalling pathway mediated by EphrinB2 promotes invasion and migration of vascular endothelial cells and lumen formation rather than inhibition of these processes.<sup>20</sup> However, the effects of the reverse signalling pathway mediated by EphrinB2 on cell migration and the specific molecular mechanism by which this may occur remain unknown. A study in the adult subventricular zone suggested that EphrinB2 signalling might regulate these processes at the

synaptic level.<sup>21</sup> All of these findings indicate that EphrinB2 expression may either directly or indirectly regulate the proliferation, differentiation and migration of neural stem cells in the subventricular zone.<sup>20</sup> EphB4 and its ligand, EphrinB2, play an important role in the development of olfactory bulb cells and migration of cerebellar granule cells.<sup>22</sup>

This current study used qPCR and Western blot to analyse the levels of EphrinB2 mRNA and protein in cells from four groups. Compared with the control and NC groups, EphrinB2 mRNA and protein levels were significantly increased in lenti-EphrinB2-BMSCs, confirming that it is possible to select and establish cell lines with stable expression. Western blot analysis demonstrated that EphrinB2 was produced in the control and NC groups, but not in the LV-shRNA-EphrinB2 group, suggesting that the shEphrinB2/BMSC line was successfully established. BMSCs are characterized by the presence of the antigens CD29 and CD90, and by the absence of CD34 and CD45. Thus, flow cytometry was performed to determine whether the cells isolated were BMSCs. The results indicated that 0.19% of cells were CD34+, 0.0% were CD45+, 92.3% were CD29+ and 99.3% were CD90+, confirming that the isolated cells were BMSCs.

In the present study, lentiviral-mediated EphrinB2/sh EphrinB2 transfection into BMSCs was performed and the effect of EphrinB2 on the differentiation of BMSCs was investigated. In previous years, research has demonstrated that BMSCs can be differentiated into neural cells under the action of appropriate inducers and cytokines *in vitro*.<sup>23</sup> The current study used neuronal cell-conditioned differentiation medium by the addition of FGF/EGF to induce BMSCs to differentiate into neuron-like cells. The current study found that the levels of specific neural markers, including MAP2, CD133 and nestin were significantly

higher in lenti-EphrinB2-BMSCs than in the control and NC groups using qPCR and immunofluorescence. The morphology of the EphrinB2/BMSCs was similar to that of neuronal cells, which suggested that EphrinB2 plays a positive role in the early differentiation of neural stem cells into neurons and their migration. Cell immunofluorescence analysis revealed that the levels of MAP2, CD133 and nestin were significantly reduced in the LV-shRNA-EphrinB2 group compared the control and NC groups. In addition, according to semi-quantitative PCR, the mRNA levels of MAP2 were significantly reduced in the LV-shRNA-EphrinB2 group compared with the control and NC groups. A previous study showed that activation of ephrin-B1 and/or ephrin-B2 molecules expressed by mesenchymal stem/stromal cells was found to increase osteogenic differentiation.<sup>24</sup> EphrinB2 expression by hippocampal astrocytes activated  $\beta$ -catenin, upregulated proneural transcription factors in neural stem cells, and thereby promoted neural differentiation through juxtacrine signalling.<sup>25</sup> A previous study suggested that stimulation of reverse EphB4-EphrinB2 signalling marginally enhanced the neural differentiation of dental pulp stem cells.<sup>6</sup> These results offer an explanation for the directional differentiation of EphrinB2/BMSCs into neuron-like cells.

To further investigate the role of EphrinB2 in regulating stem cell migration, the current study used a transwell assay to detect cell migration in each group. The number of migrated cells was significantly higher in lenti-EphrinB2-BMSCs than in the control and NC groups. In addition, an inhibitory effect of EphrinB2 suppression by siRNA knockdown on the migration was observed. These results suggest that EphrinB2 can increase the ability of cells to migrate *in vitro* and confirmed the important role that the *Efnb2* gene plays in regulating BMSC migration.

The EphB4/EphrinB2 reverse signalling pathway has been reported to participate in the differentiation of mesenchymal stem cells into cardiocytes.<sup>26,27</sup> The SH2/SH3 adaptor protein Grb4 has been implicated as a molecular bridge that connects the tyrosine phosphorylated EB3 cytoplasmic tail with the Dock180 guanine nucleotide exchange factor, Rac activation, and the downstream effector PAK to mediate axon retraction and pruning.<sup>7</sup> To elucidate the mechanism underlying this action, this current study evaluated the phosphorylation of key kinases in the PAK pathway in stably transduced BMSCs. EphrinB2 upregulation activated PAK, suggesting that EphrinB2 might activate PAK by modulating Grb4 in BMSCs. Taken together, these data indicate that EphrinB2 promotes BMSC migration by regulating the EphB4/EphrinB2 reverse signal pathways. At present, little is known about the function of EphrinB2 and the Eph family in stem cells. With the development of molecular biological technologies, research on the molecular mechanism underlying neural stem cell differentiation into neurons will advance. In the future, it may be possible to control the differentiation of neural stem cells artificially and to induce directional differentiation that may allow clinical application of neural stem cells.

In conclusion, EphrinB2 can promote the differentiation and migration of rat BMSCs. The findings of this study suggest that the EphB4/EphrinB2 reverse signalling pathway plays an important role in regulating BMSC migration. In the future, it will be important to study the mechanism of EphB4/EphrinB2 regulation of BMSCs and to establish theoretical and experimental frameworks to identify effective targets of gene therapy.

#### Declaration of conflicting interest

The authors declare that there are no conflicts of interest.

#### Funding

This study was supported by grants awarded to Min Zhu from the National Natural Science Foundation of China (no. 81401864) and the Science and Technology Development Fund Project of Nanjing Medical University of China (no. 2013NJMU097).

#### ORCID iD

Min Zhu  <https://orcid.org/0000-0002-9317-8363>

#### References

1. Kodera Y. Recent advances of transplantation from bone marrow derived stem cells. *Nihon Rinsho* 2011; 69: 2179–2185 [In Japanese, English abstract].
2. Borlongan CV, Glover LE, Tajiri N, et al. The great migration of bone marrow-derived stem cells toward the ischemic brain: therapeutic implications for stroke and other neurological disorders. *Prog Neurobiol* 2011; 95: 213–228.
3. Genander M and Frisén J. Ephrins and Eph receptors in stem cells and cancer. *Curr Opin Cell Biol* 2010; 22: 611–616.
4. Wang Y, Thorin E, Luo H, et al. EPHB4 protein expression in vascular smooth muscle cells regulates their contractility, and EPHB4 deletion leads to hypotension in mice. *J Biol Chem* 2015; 290: 14235–14244.
5. Yang JS, Wei HX, Chen PP, et al. Roles of Eph/ephrin bidirectional signaling in central nervous system injury and recovery. *Exp Ther Med* 2018; 15: 2219–2227.
6. Heng BC, Gong T, Xu J, et al. EphrinB2 signalling modulates the neural differentiation of human dental pulp stem cells. *Biomed Rep* 2018; 9: 161–168.
7. Xu NJ and Henkemeyer M. Ephrin-B3 reverse signaling through Grb4 and cytoskeletal regulators mediates axon pruning. *Nat Neurosci* 2009; 12: 268–276.
8. Lu Q, Sun EE, Klein RS, et al. Ephrin-B reverse signaling is mediated by a novel PDZ-RGS protein and selectively inhibits G protein-coupled chemoattraction. *Cell* 2001; 105: 69–79.

9. Alam SM, Fujimoto J, Jahan I, et al. Coexpression of EphB4 and ephrinB2 in tumour advancement of ovarian cancers. *Br J Cancer* 2008; 98: 845–851.
10. Li M, Yu A, Zhang F, et al. Treatment of one case of cerebral palsy combined with posterior visual pathway injury using autologous bone marrow mesenchymal stem cells. *J Transl Med* 2012; 10: 100.
11. Bochenek ML, Dickinson S, Astin JW, et al. Ephrin-B2 regulates endothelial cell morphology and motility independently of Eph-receptor binding. *J Cell Sci* 2010; 123: 1235–1246.
12. Aoto J and Chen L. Bidirectional ephrin/Eph signaling in synaptic functions. *Brain Res* 2007; 1184: 72–80.
13. Pasquale EB. Eph-ephrin bidirectional signaling in physiology and disease. *Cell* 2008; 133: 38–52.
14. Sentürk A, Pfennig S, Weiss A, et al. Ephrin Bs are essential components of the Reelin pathway to regulate neuronal migration. *Nature* 2011; 472: 356–360.
15. De Bellard ME, Ching W, Gossler A, et al. Disruption of segmental neural crest migration and ephrin expression in delta-1 null mice. *Dev Biol* 2002; 249:121–130.
16. Wilkinson DG. Multiple roles of EPH receptors and ephrins in neural development. *Nat Rev Neurosci* 2001; 2:155–164.
17. Jevince AR, Kadison SR, Pittman AJ, et al. Distribution of EphB receptors and ephrin-B1 in the developing vertebrate spinal cord. *J Comp Neurol* 2006; 497: 734–750.
18. Cramer KS, Karam SD, Bothwell M, et al. Expression of EphB receptors and EphrinB ligands in the developing chick auditory brainstem. *J Comp Neurol* 2002; 452: 51–64.
19. Kemmerling N, Wunderlich P, Theil S, et al. Intramembranous processing by  $\gamma$ -secretase regulates reverse signaling of ephrin-B2 in migration of microglia. *Glia* 2017; 65: 1103–1118.
20. Hamada K, Oike Y, Ito Y, et al. Distinct roles of ephrin-B2 forward and EphB4 reverse signaling in endothelial cells. *Arterioscler Thromb Vasc Biol* 2003; 23: 190–197.
21. Conover JC, Doetsch F, Garcia-Verdugo JM, et al. Disruption of Eph/ephrin signaling affects migration and proliferation in the adult subventricular zone. *Nat Neurosci* 2000; 3: 1091–1097.
22. Arthur A, Koblar S, Shi S, et al. Eph/ephrinB mediate dental pulp stem cell mobilization and function. *J Dent Res* 2009; 88: 829–834.
23. Woodbury D, Schwarz EJ, Prockop DJ, et al. Adult rat and human bone marrow stromal cells differentiate into neurons. *J Neurosci Res* 2000; 61: 364–370.
24. Arthur A, Zannettino A, Panagopoulos R, et al. EphB/ephrin-B interactions mediate human MSC attachment, migration and osteochondral differentiation. *Bone* 2011; 48: 533–542.
25. Ashton RS, Conway A, Pangarkar C, et al. Astrocytes regulate adult hippocampal neurogenesis through ephrin-B signaling. *Nat Neurosci* 2012; 5: 1399–1406.
26. Jahn T, Seipel P, Coutinho S, et al. Grb4/Nckbeta acts as a nuclear repressor of v-Abl-induced transcription from c-jun/c-fos promoter elements. *J Biol Chem* 2001; 276: 43419–43427.
27. Liu H, Devraj K, Möller K, et al. EphrinB-mediated reverse signalling controls junctional integrity and pro-inflammatory differentiation of endothelial cells. *Thromb Haemost* 2014; 112: 151–163.